Model-based ammonia slip observation for SCR control and diagnosis

Carlos Guardiola, Benjamín Pla, Pau Bares, and Javier Mora,

Abstract—The control and diagnosis of selective catalytic reduction (SCR) system require from a precise estimation of NOx reduction in order to properly control the NH_3 injection. This paper aims to resolve the cross-sensitivity of current NOx sensors at the outlet of the SCR, by providing the control unit with an estimation of NOx and ammonia slip.

The problem of discerning between NOx and ammonia slip is solved by identifying an intermediate variable representing the SCR load. The SCR load is estimated by combining the mass conservation principle between the inlet and the outlet of the SCR and a NOx reduction model, via an Extended Kalman filter. Current models and observers have several limitations to represent the real behaviour of the SCR along all the operating conditions: on one hand, when relying on the mass conservation, small errors at models are integrated, leading to important bias on the SCR load, on the other hand, the dynamics at the SCR difficult the observation and the adaptation of the model. The main focus of the developed algorithm is to use a simplified model which might be used for ammonia slip estimation, being aware of current limitations of SCR models in real operation.

Experimental results in a EURO 6 compression ignited (CI) engine show the potential of such observation in transient conditions and an adequate correlation with external ammonia measurements provided by additional sensors available on the test bench.

Index Terms—Diesel engine emissions, SCR, NOx sensor, cross-sensitivity, Kalman filter

I. INTRODUCTION

Regulation requirements are evolving to meet society needs for a low polluted atmosphere [1]. For this purpose, new regulation procedures use portable emissions measurement systems (PEMS) in real driving emissions (RDE) conditions for type-approval procedures[1]. In this line, diesel after-treatment systems (ATS) have evolved to reduce pollutant emissions below regulation thresholds [2]. Specifically, selective catalytic reduction (SCR) systems allow reducing engine-raw NO_x emissions, with the injection of ammonia (NH_3) in the exhaust line. However, due to the own SCR operation characteristics, NO_x and NH_3 species may slip from the catalyst [3], [4]. Then, measuring these species slip on-board is relevant to keep emissions below the admitted threshold.

On-board sensors are required for control and on-board diagnostics (OBD), as it is the case of the SCR downstream NO_x sensor [5], [6], [7], [8]. Specifically, this sensor is, for closed-loop control of deNO$_x$ systems, required to meet Euro

C. Guardiola, B. Pla, P. Bares and J. Mora work at Universitat Politècnica de València, 46022 Spain (corresponding author e-mail: pabamo@mot.upv.es).

6 emission targets [9]. However, it presents cross-correlation with NH_3 [10], [11]. Therefore, NO_x and NH_3 signals must be decoupled from the sensor measurement, or it could lead, for instance, to instabilities in closed-loop control, if NH_3 slip is considered as NO_x slip. A NH_3 sensor could allow the NO_x signal reconstruction [12], [13], [14], although depending on the vehicle segment, the inclusion of the NH_3 sensor may be expensive [15]. Then, the aim of this article is to isolate both NO_x and NH_3 signals from the NO_x sensor measurement, without the use of an on-board NH_3 sensor measurement and by means of a Kalman filter.

Several configurations can be found in an after-treatment system with regards to blocks and sensors [16], [17], [18], [19]. In this sense, a diesel oxidation catalyst (DOC) or passive NO_x adsorber (PNA) are usually placed in front of the exhaust line, while diesel particulate filters (DPF) and deNO$_x$ reduction systems can be found in [20]. In case an SCR is present, as it is the case of this work, an injector is placed upstream the SCR to inject an NH_3-based solution [21], [22]. Then, for the purpose of this article, both SCR up- and downstream NO_x signals are considered available, while the downstream NH_3 signal will be used to provide the NH_3 slip, only for the algorithm calibration and validation.

Some works can be found in literature concerning SCR model approaches, from detailed 1D models to control-oriented 0D models [23], [24], [25], [26], [27]. These models capture the different dynamics present in an SCR [28], [25]. While NO_x slip follow the upstream NO_x dynamics, the NH_3 slip dynamics are slower, since its dynamics are similar to the catalyst NH_3 storing capacities [29], [30]. The use of an open loop SCR model is restricted to track the NH_3 loading state of the SCR. In this sense, if for any reason like sensor excursions or model inaccuracies, the SCR load (θ) is biased with regards to the actual value, the model will be inaccurate until the actual SCR load returns to a known value, which can be an empty state of the catalyst. Then, this problematic points out the need for updating this state through an observer.

Several works have been focused on designing optimal observers for the estimation of the NH_3 and NO_x slip by using simulations for validation purposes. Some examples can be found in [31] with a Newton observer, in [32] with a Lyapunov-based observer, or in [33], [34], [35] with an Extended Kalman Filter. Specially remarkable is the work of Zhang et al., which is focused on the observation of the operation of single-cell [36], [37] and double-cell [38], [39]

SCR systems by designing Luenberg-like observers with SCR models based in three states, namely ammonia and NOx concentrations, and SCR coverage ratio, and by assuming pre-calibrated cross-sensitivity as a function of the temperature.

The observer presented in this work analyses sensor signals that can be found nowadays in vehicles, i.e. inlet and outlet NO_x, NH_3 injection estimation, temperature, pressure and exhaust mass flow, and estimates an intermediate state that represents the SCR load to discern between NH_3 and NO_x slip. In contrast with previous works, here an observer with a single state (the SCR load) is modelled by analysing the emptying and filling dynamics of the SCR, and a variable update of the state from a NOx conversion model is proposed by using an EKF with variable noise. The SCR load is updated faster when no NOx is measured at the inlet of the SCR and hence all NOx measured at the outlet can be assumed ammonia slip caused by sensor cross-sensitivity.

The presented model makes use of several hypothesis in order to capture the main characteristics of the SCR but taking into account the existing limitations in real operating conditions, such as variable cross-sensitivity, or inaccurate prediction of NO_x sensor and transport dynamics. Furthermore its computational burden is low and its linearization facilitates the Kalman filter state space with limited associated errors. The developed algorithm has been validated with experimental data and had shown the potential to be implemented in real time applications for control and diagnosis purposes.

II. EXPERIMENTAL SET-UP

Experimental tests were carried out in a dynamic engine test bench, to which a turbocharged 1.5l common-rail direct injection Euro 6 Diesel engine was coupled. The engine has an intercooled exhaust gas recirculation (EGR) valve and a variable geometry turbine (VGT), whose relevant characteristics are summarized in Table I.

TABLE I: PSA dV5 Engine main characteristics.

Stroke (S) x Bore (D)	84.8 x 75 mm
Number of cylinders (z)	4
Displacement	1498 cc
Compression ratio	16:1
Maximum torque	300 Nm @ 1750 rpm
Emission standard	Euro 6

The engine ATS is composed of a compacted unit with DOC, SCR and SCR filter (SCRF), where the mixing chamber for the NH_3 injection is located between the DOC and the SCR. The Horiba Dyno3 engine bench was controlled with a STARS system, i.e. an automation system provided by Horiba for running a wide range of Test Programs from simple manual testing to dynamic automatic tests, to which several temperature and pressure measurements along the exhaust line were connected. An image of the engine test bench and the instrumented after-treatment system is shown in Figure 1.

A hardware-in-the-loop system was implemented in the test bench, in order to perform the real time signal separation

Fig. 1: Image of the engine (left) and after-treatment system (right).

strategy with a dSpace microautobox II rapid prototyping system. Then, the prototyping system was connected to an ETAS 910, which was connected to the electronic control unit (ECU) of the engine and allowed to perform bypass control. In this sense, while the NOx sensors were connected to the ECU, the NH_3 sensor was connected to the prototyping system.

The necessary signals to execute the algorithm are the exhaust mass flow, the temperature and pressure of the exhaust gases, the inlet NOx signal, the outlet NOx signal and the NH_3 injection flow, while the NH_3 sensor was used only for calibration and to validate the strategy performance. Figure 2 shows an scheme of the engine and after-treatment layout, where the relevant systems and sensors have been highlighted.
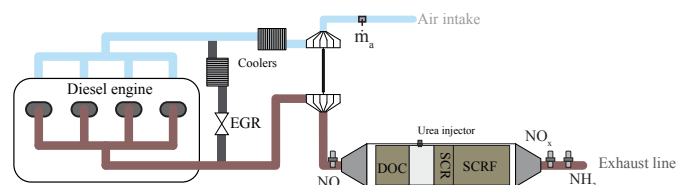

Fig. 2: Experimental test bench engine and after-treatment system layout.

Various tests were carried out in the engine with variable NH_3 dosing and by varying the engine operating conditions. In this paper, only three tests will be shown to illustrate the characteristics of the developed approach: two training tests, one at low and other at high temperature, and a validation test, which consists in a World Harmonized Light-Duty Test Procedure (WLTP) cycle. Figure 3 shows the temperature (top plots), mass flow (middle plots), and inlet NOx (bottom plots) of three aforementioned tests.

III. METHOD DESCRIPTION

The presented methodology designs a Kalman filter that makes use of a simplified 0D model, which is able to capture the main features of the SCR system but has low
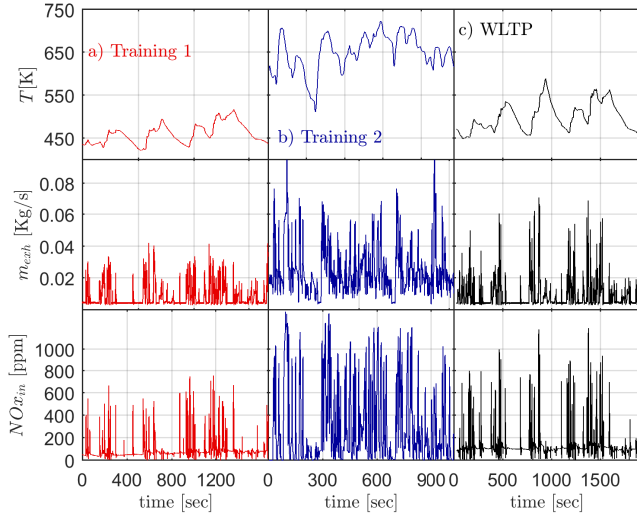
Fig. 3: Temperature (top), mass flow (middle), and inlet NOx (bottom) of three tests used to analyse the algorithm: a) training dataset at low temperature, b) training dataset at high temperature, and c) WLTP cycle.

computational burden and is suitable for being linearized.

SCR model: The SCR model used in the current approach is based on four hypothesis.

1) The cross sensitivity, that evaluates which is the influence of the NH_3 slip on the outlet NOx measurement, can be represented by a constant value of 0.67, such as suggested in [11]. The sensors used in the present paper have been evaluated at various operating conditions, showing a cross-sensitivity close to that value.

$$NOx_{SS} = NOx_{out} + 0.67 NH3_{out} \qquad (1)$$

where NOx_{SS} is the outlet NOx measurement, NOx_{out} the NOx slip, and $NH3_{out}$ the NH_3 slip.

2) The mass conservation can be applied between the inlet and the outlet of the SCR to estimate its load (θ).

$$\frac{\delta\theta}{\delta t} = (NH3_{in} - \Delta NOx - NH3_{out}) \qquad (2)$$

where $NH3_{in}$ is the the NH_3 absorbed by the SCR, and ΔNOx the NH_3 used for NOx conversion. The model assumes that 1 ppm of NH_3 is used to convert 1 ppm of NOx, and considers that all the NH_3 injected is absorbed by including its dynamics at the desorption process. The NOx used for conversion can be also rewritten as:

$$\Delta NOx^k = NOx_{in}^k - NOx_{SS}^k + 0.67 NH3_{out}^k \qquad (3)$$

3) The NOx variations along the SCR volume (δV) and over the time (δt) are proportional to the existing NOx in the SCR, and the SCR load, with a proportional value which depends on the temperature, following:

$$\frac{\delta^2 NOx}{\delta t \delta V} = NOx\theta f_2'(T) \qquad (4)$$

where the influence of the temperature, $f_2'(T)$, use to be represented by an Arrhenius function, such as in [23]. This equation is composed from an exponential function of the SCR load and the residence time when it gets discretized, such as:

$$NOx_{out} = NOx_{in}e^{-\theta f_2(T)\Delta t} \qquad (5)$$

where Δt is the residence time, and $f_2(T)$ represents the effect of the temperature.

4) The NH_3 slip is proportional to the SCR load and the mass flow, and the proportional value is function of the temperature:

$$NH3_{out} = m_{exh}\theta f_1(T) \qquad (6)$$

where θ is the SCR load, $f_1(T)$ represents the effect of the temperature, which is expected to have an Arrhenius-like shape, m_{exh} the mass flow, and T the temperature of the gases.

Other SCR models such as [23] or [26] make use of a maximum SCR load to model the absorption and desorption of the SCR in order to maintain the SCR load under desired levels even in the case of a possible a model bias. In this work a simplified expression of the NH_3 slip has been chosen to facilitate the linearisation and use of such model in a Kalman filter and because the SCR load will be continuously updated during the operation, avoiding a possible integration of errors in terms of bias in the SCR load.

The residence time in the SCR (Δt) has been calculated by integrating the instantaneous speed (V_{exh}) until the length of the SCR (L_{SCR}) is reached:

$$L_{SCR} = \int_t^{t=t+\Delta t} V_{exh}(t)dt \qquad (7)$$

where the instantaneous speed is computed by assuming an average frontal area of the SCR ($A_f = \pi D_{SCR}^2/4$), and by obtaining the instantaneous density (ρ) from the exhaust temperature (T) and pressure (p_{exh}):

$$V_{exh} = \frac{m_{exh}}{\rho A_f} = \frac{m_{exh}4RT}{p_{exh}\pi D_{SCR}^2} \qquad (8)$$

where R is the constant of the gases ($R \approx 287J/KgK$).

An adequate identification of the residence time through D_{SCR} and L_{SCR} is important to study the NOx conversion, i.e. the inlet NOx signal must be delayed in order to be compared with the outlet NOx measurement. The top plot of Figure 4 shows the residence time obtained during a transient by using $D_{SCR} = 11cm$ and $L_{SCR} = 1.4m$, and the bottom plot of the Figure shows the inlet NOx raw signal (NOx_{in}^{raw}), the inlet signal delayed (NOx_{in}) and the outlet NOx signal (NOx_{out}).

The aim of the Kalman filter is the observation of an intermediate state, the SCR load, in order to distinguish the
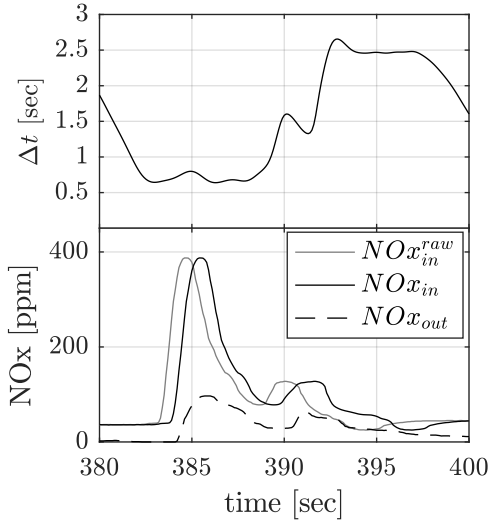
Fig. 4: Residence time and NOx signals obtained in a transient.

NH_3 and the NOx slip in the outlet NOx sensor. In fact, the Kalman filter combine two sources of information, with different dynamic characteristics:

- The mass conservation: It estimates the evolution of the NH_3 load by analysing the inlet and outlet measurements. When combining Equation (2), with the NH_3 slip assumption, Equation (6), and the cross-sensitivity, Equation (1), it leads to:

$$\theta^{k+1} = \theta^k + dt[NH3_{in}^k - NOx_{in}^k + NOx_{SS}^k \\ -1.67\theta^k m_{exh}^k f_1(T^k)] \qquad (9)$$

Here, all the units are used in the international system. Sensors commonly use ppm for the signal output, however, the conversion is direct when using the mass flow and the molecular weights:

$$NOx[Kg/s] = NOx[ppm]\frac{17}{29}m_{exh}[Kg/s] \qquad (10)$$

- A NOx conversion model: The model of NOx conversion can be used in combination of the inlet and outlet NOx measurement to determine which is the SCR load that fits the NOx conversion. From Equations (1) and (5):

$$NOx_{SS}^k = NOx_{in}^k e^{-\theta^k f_2(T^k)\Delta t^k} + 0.67\theta^k m_{exh}^k f_1(T^k) \qquad (11)$$

It must be remarked that if the inlet NOx are negligible the NOx conversion model is not used, leading to:

$$NOx_{SS}^k = 0.67\theta^k m_{exh}^k f_1(T^k) \qquad (12)$$

Note that in Equation (9) the NOx conversion model is not used, but analyses the inlet and outlet measurements during the last cycles for characterizing the emptying and filling of the SCR, while Equation (11) gives an instantaneous estimation of the SCR load that would fit the NOx conversion model, but it does not use the injected NH_3. On the one hand, the mass conversion might predict the dynamics of the SCR load evolution but might integrate a bias in the model ending up with an inadmissible error prediction, which would lead to significant errors in the final ammonia slip and NOx conversion efficiency estimation. On the other hand, the value given by the NOx reduction model offers a value of SCR load at each time lapse, but small errors in the model, in the signals or in the dynamics of the signals, might be amplified leading to high noise measurement.

To combine these two sources of information a Kalman filter with one state and one measurement is used, being the state the SCR load (θ), and the output the outlet NOx sensor measurement (NOx_{SS}). The state representation can be defined by:

$$\theta^{k+1} = f(\theta^k, u^k) + w^k \qquad (13)$$
$$NOx_{SS}^k = g(\theta^k, u^k) + v^k \qquad (14)$$

where u are the inputs that define the system in a given step k, w the associated noise to the state equation, and v the noise associated to the output estimation.

Extended Kalman filter: The KF of the state vector is defined by:

$$\hat{\theta}^{k|k-1} = f(\hat{\theta}^{k-1}, u^k) \qquad (15)$$
$$\varepsilon^k = NOx_{SS}^k - g(\hat{\theta}^{k|k-1}, u^k) \qquad (16)$$
$$\hat{\theta}^k = \hat{\theta}^{k|k-1} + K^k \varepsilon^k \qquad (17)$$

The KF is characterized for minimizing the expected estimation error by solving an iterative Riccati equation and updating the value of the Kalman gain (K). Following:

$$P^{k|k-1} = (d\theta^k P^{k-1} d\theta^k + w^k) \qquad (18)$$
$$K^k = P^{k|k-1} dNOx_{SS}^k \\ (dNOx_{SS}^k P^{k|k-1} dNOx_{SS}^k + v^k)^{-1} \qquad (19)$$
$$P^k = (1 - K^k dNOx_{SS}^k)P^{k|k-1} \qquad (20)$$

where the derivatives of the system ($d\theta^k$ and $dNOx_{SS}^k$) can be obtained by linearising equations 9 and 11 with respect to θ, such as:

$$d\theta^k = 1 - 1.67 dt f_1(T^k)m_{exh}^k \qquad (21)$$
$$dNOx_{SS}^k = 0.67 f_1(T^k)m_{exh}^k \\ -NOx_{in}^k f_2(T^k)\Delta t^k e^{-\theta^k f_2(T^k)\Delta t^k} \qquad (22)$$

The associated noises (w^k and v^k), have been selected to follow the mass conservation but with a slight update when NOx is being converted and a fast update, when no NOx is converted ($NO_{in} \approx 0$).

IV. CASE STUDY

Model Calibration: The function f_1 characterizes how fast is filled and emptied the SCR at a given temperature. Figures 5 and 6 show the effect of the parameters in the first training data set (with an average temperature of 450K). The numerical values strongly depend on the operating conditions, for these concrete operating condition, i.e. this part of the first training dataset, the average values of f_1 and f_2 are 0.05 and 3.02 e4 respectively, and the model output is 46 ppm of average urea slip and 102 ppm of average NOx slip.
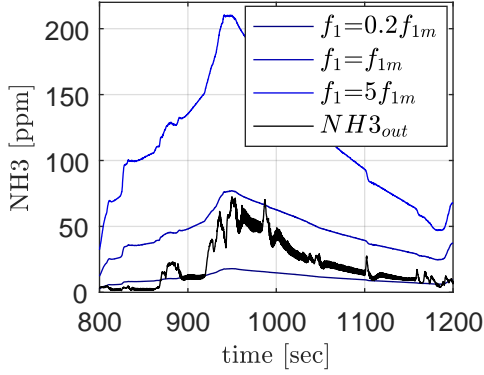

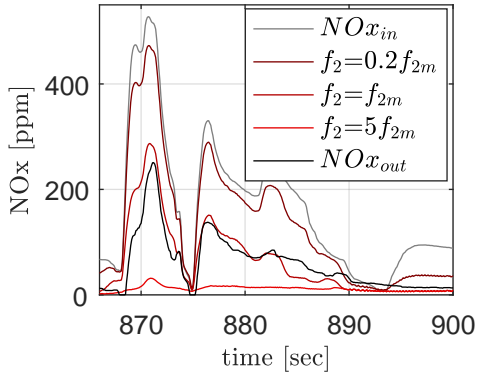Fig. 5: Part of first training dataset where the model is used with various values of f_1.

Fig. 6: Part of first training dataset where the model is used with various values of f_2.

Figure 5 shows the measured NH$_3$ slip, the result of the model when applying the calibrated value (f_{1m}), and the effect of reducing and augmenting the parameter per five. When augmenting the value of f_1, the absorption and desorption of NH$_3$ is accelerated, and hence the dynamics are faster. Concretely, if f_1 is multiplied by 0.2 the model would estimate an average urea slip of 10 ppm, while if it is increased 5 times, the final average urea slip would be 128 ppm.

Figure 6 shows the effect of varying the parameter f_2. When this parameter is low, such as in the first case, there is little NOx conversion and the final NOx value given by the model is close to the NOx_{in} (154 ppm in this case), but when the value is too high, such as in the third case, the

conversion of NOx is amplified and hence the final value is always close to zero (31 ppm in this case).

The effect of the temperature on f_1 and f_2 is commonly simulated with Arrhenius function. However in this paper a 1D look-up-table has been preferred. A 1D look-up-table allows capturing the effect of the temperature, even with non-linear behaviour, such as in an Arrhenius function, but gives more freedom to the function and simplifies the calibration procedure for a final on-board application.

The calibration procedure proposed can be summarized in a six step procedure. For identifying the dynamics of the SCR slip, an external measurement of NH$_3$ slip, provided by a test-bench sensor or other models, must be used:

1) The exhaust operating conditions (air mass flow and the engine-out NOx) are varied by maintaining the temperature almost constant.
2) The value of f_1 is obtained by minimizing the error in NH$_3$ slip, optimizing:

$$\varepsilon(NH3) = |NH3_{out} - m_{exh}\theta f_1| \qquad (23)$$

Note that for f_1 calibration, only the mass conservation, Equation (9), and hence the emptying and filling dynamics, are considered.

3) Once f_1 is estimated, now the experimental SCR load (θ_{exp}) is obtained from the experimental NH$_3$ measured, such as:

$$\theta_{exp} = \frac{NH3_{out}}{m_{exh}f_1} \qquad (24)$$

4) Next step is based on finding f_2 by minimizing the error in the outlet NOx sensor

$$\varepsilon(NOx) = |NOx_{SS} - (NOx_{in}e^{-\theta_{exp}f_2\Delta t} + 0.67m_{exh}\theta_{exp}f_1)| \qquad (25)$$

5) Then the procedure is repeated at various temperatures to find the curves $f_1(T)$ and $f_2(T)$.
6) As it is difficult to obtain experimental data with significant variations of exhaust mass, outlet NOx, and SCR load at constant temperature, once the first curves are found, a second calibration procedure is proposed. In this second calibration, the full curves will be used multiplied by a constant value (x_1 and x_1), to take into account the variations during the test, following:

$$\varepsilon(NH3) = |NH3_{out} - m_{exh}\theta x_1 f_1(T)| \qquad (26)$$
$$\varepsilon(NOx) = |NOx_{SS} - (NOx_{in}e^{-\theta_{exp}x_2 f_2(T)\Delta t} + 0.67m_{exh}\theta_{exp}x_1 f_1(T))| \qquad (27)$$

Figure 7 shows the result of the calibration for the SCR analysed. Note that the final function is similar to an Arrhenius function, which is in line with other modelling works.

Regarding the noise associated to the state transition and the observation model, namely w and v, a variable noise has been used to consider different state update rates when the NOx
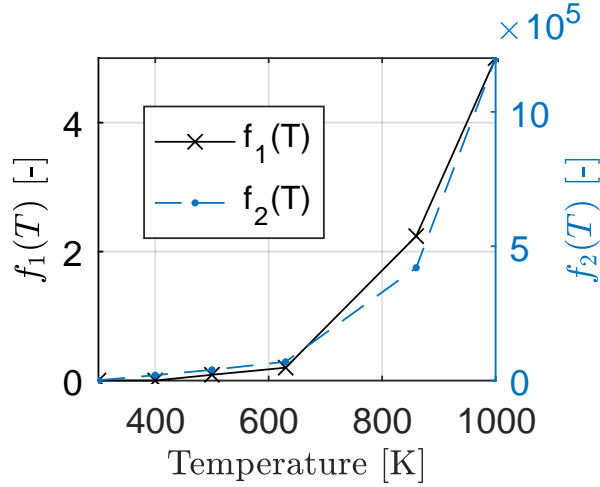
Fig. 7: Model calibration of $f_1(T)$ and $f_2(T)$.

Fig. 8: EKF result of the first training dataset when using various values of w: thick red line shows the NH3 measurement and dashed line shows the output of the model without adaptation.

model is not taking part in the equations.

The noise associated to the observation model (v) when there is 0 NOx at the inlet of the SCR (and hence all the outlet NOx measured can be considered NH_3) is 5 ppm, while a value of 35 ppm has been used when the inlet NOx is above 30 ppm and hence some NOx reduction is assumed. In between, i.e. from 0 to 30 ppm, a variable noise was used to take into account the uncertainty of the NOx sensor, such as:

$$v_k = \begin{cases} NOx_{in}^k + 5 & \text{if } NOx_{in}^k < 30 \\ 35 & \text{if } NOx_{in}^k \geq 30 \end{cases} \quad (28)$$

A value of 1 mg has been selected for the noise associate to the state transition model, as a trade-off between a fast adaptation and robustness. Figure 8 shows the result of the EKF when using various values for the noise associated to the state transition model. Three values of w have been represented with various colour intensities, a thick red line shows the NH3 measurement and dashed line shows the output of the model without adaptation.

Note that a small value of w ($w < 0.1$mg) makes the EKF rely more on the mass conservation, while a high value of w ($w > 10$mg) forces a fast adaptation relying on the NOx conversion model. The effect of v is somehow opposite to that of w, i.e. if v is increased, the EKF would rely more in the mass conservation (same effect than reducing w).

The NOx sensor at the outlet is used to provide the most likely SCR load for the given measurement. Nevertheless, there are always two possibilities: either everything is urea slip detected by the cross-sensitivity, and hence the estimated SCR load is high, or the outlet NOx measured is a combination of both, urea and NOx slip, and the SCR load is lower. The objective of the EKF is to use the mass conservation and other inputs to provide the system with an adequate adaptation of the SCR load. Although a fast adaptation is sometimes desired
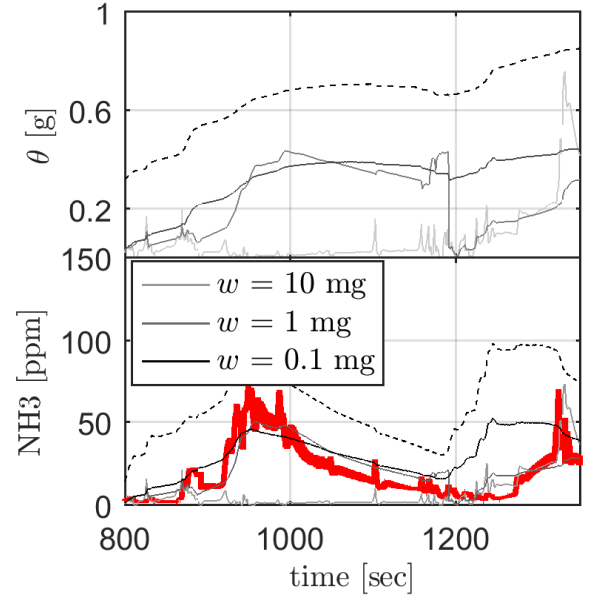
to eliminate the bias, because of the different dynamics on the signals acquired and the model errors, the robustness of the estimation might be in danger.

One of the strengths of the EKF is its robustness to perturbations at the inputs. The use of an adaptation through the outlet NOx sensor allows the EKF to correct errors at the urea injected, at the inlet NOx or at the mass flow sensor, while using mass conservation allows the algorithm to avoid spikes caused by incorrect phasing at the outlet NOx measurement. Only an error in the cross-sensitivity error is directly propagated at the urea slip estimation but does not affect the overall performance of the algorithm.

V. RESULTS AND DISCUSSION

Figure 9 shows the NH_3 sensor output (with a thick red line), the result of the model (with a dashed grey line), and the result of the Kalman filter (with a continuous black line) in the three tests shown in Figure 3. As it is shown, the dynamics of the measured NH_3 slip is followed by the model, however a bias is produced during the tests as the model is based on the past measurements and not only the current measured signals. As consequence the NOx output of the model when using the modelled SCR load does not perfectly correlate with the NOx sensor output. The bias is corrected when using the Kalman filter with the measurement provided by the NOx sensor and a NOx conversion model to update the SCR load.

The error of the SCR model, calculated as the absolute value of the differences with the NH_3 sensor, i.e. Equation (23), is 26.65, 57.13, and 66.35 ppm, for the three tests,
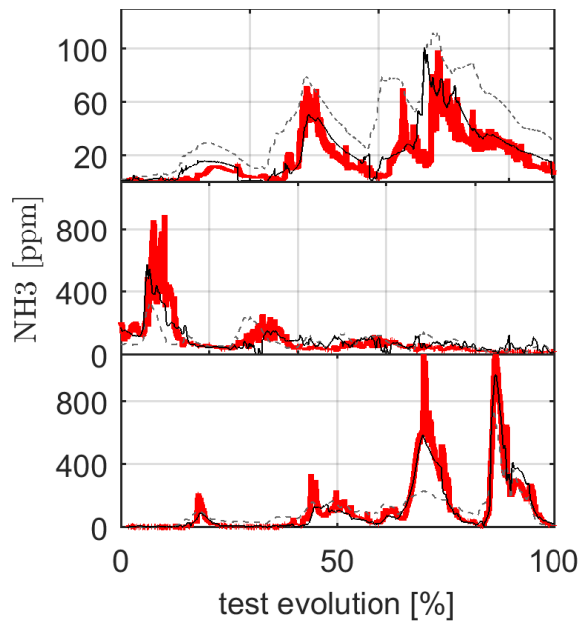
Fig. 9: NH$_3$ slip in the three tests: training dataset at low temperature (top plot), training dataset at high temperature (medium plot), and WLTP cycle (bottom plot). A thick red line shows the NH3 measurement, a black line shows the output of the EKF and a dashed grey line shows the model result without adaptation.
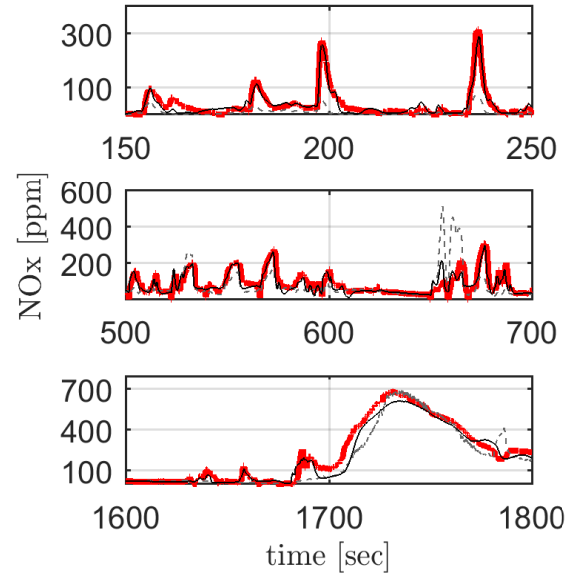

Fig. 10: NOx sensor reading in the three tests: training dataset at low temperature (top plot), training dataset at high temperature (medium plot), and WLTP cycle (bottom plot). A thick red line shows the NH3 measurement, a black line shows the output of the EKF and a dashed grey line shows the model result without adaptation.

which have an average NH$_3$ measured slip of 17.71, 88.24 and 121.94 ppm. When applying the Kalman filter the error is reduced to 7.9, 41 and 32.6 ppm at each test, that implies an error reduction of 70%, 40%, and 50% for the three tests.

Figure 10 shows the measured NOx at the outlet (with a thick red line), the result of the model (with a dashed grey line), and the output of the Kalman filter (with a continuous black line) in a given range. The modelled NOx seems to correlate with the experimental results, however predicted NOx are underestimated or overestimated because of the bias at the SCR load. The Kalman filter follows the NOx measurement by using the error between the model and the outlet NOx sensor to correct a possible bias that might be integrated at past cycles.

VI. CONCLUSIONS

NH$_3$ injection in current SCR systems is based in a control scenario based on the inlet and outlet NOx sensor measurements. However, in order to use these sensors for an adequate NH$_3$ injection strategy, an estimation of the NOx and the NH$_3$ slip, must be provided. Current SCR models determine the NOx and NH$_3$ slip based on the SCR load and predict the SCR load by using the mass conservation at the inlet and oultet of the SCR to analyse the accumulation of NH$_3$. Nevertheless, these models use to exhibit significant errors when the initial SCR load is not known, or when model or sensor bias are integrated.

The present paper proposes a simplified model oriented to control applications which provides a measurement of the NH$_3$ slip based on an intermediate state which represents the SCR load. The approach makes use of two sources of information to predict the SCR load: the mass conservation to determine the evolution of the SCR load and a model of the NOx conversion efficiency to analyse which is the most likely value of SCR load at each time lapse.

A Kalman filter is used to combine both measurements by modelling the dynamics of the SCR load with the mass conservation principle and by updating the current model in two levels: with a slow update when NOx are converted, and consequently a significant error can be expected from the NOx conversion, and a fast update when no NOx are converted, and hence all the NOx measured at the outlet NOx sensors are mainly NH$_3$ slip.

An external NH$_3$ measurement was used to validate the proposed methodology with experimental data. Using a Kalman filter implies an error reduction of 70%, 40%, and 50% for the three tests shown, when comparing with the results of the model. The presented approach has the potential of predicting the NH$_3$ slip, not only qualitatively, but also to quantify it. Future works will be focused on the possibility of an online adaptation of SCR models to consider ageing factor or different exhaust lines, and the use of such measurement for SCR control purposes.

REFERENCES

[1] F. Posada and J. German, "Review of LDV OBD requirements under the European, Korean and Californian emissions programs," *The international council on clean transportation*, 2016.

[2] T. Johnson and A. Joshi, "Review of vehicle engine efficiency and emissions," in *WCX 17: SAE World Congress Experience 2017-01-0907*. SAE International, mar 2017.

[3] Z. Skaf, T. Aliyev, L. Shead, and T. Steffen, "The state of the art in selective catalytic reduction control," in *SAE 2014 World Congress & Exhibition 2014-01-1533*. SAE International, 2014.

[4] J. Riegel, H. Neumann, and H.-M. Wiedenmann, "Exhaust gas sensors for automotive emission control," *Solid State Ionics*, vol. 152, pp. 783–800, 2002.

[5] Y.-Y. Wang, Y. Sun, C.-F. Chang, and Y. Hu, "Model-based fault detection and fault-tolerant control of scr urea injection systems," *IEEE Transactions on Vehicular Technology*, vol. 65, no. 6, pp. 4645–4654, 2016.

[6] R. Chen and X. Wang, "Model-based fault diagnosis of selective catalytic reduction systems for diesel engines," *SAE Int. J. Passeng. Cars - Electron. Electr. Syst. 2014-01-0280*, vol. 7, pp. 449–453, 04 2014.

[7] D. Upadhyay and M. Van Nieuwstadt, "Model based analysis and control design of a urea-SCR deNOx aftertreatment system," *Journal of dynamic systems, measurement, and control*, vol. 128, no. 3, pp. 737–741, 2006.

[8] M. Van Nieuwstadt and D. Upadhyay, "Diagnosis of a urea scr catalytic system," Patent, 9, 2005, uS Patent 6.925.796.

[9] F. Willems, R. Cloudt, E. van den Eijnden, M. van Genderen, R. Verbeek, B. de Jager, W. Boomsma, and I. van den Heuvel, "Is closed-loop SCR control required to meet future emission targets?" in *SAE Technical Paper Series 2007-01-1574*. SAE International, apr 2007.

[10] A. Bonfils, Y. Creff, O. Lepreux, and N. Petit, "Closed-loop control of a scr system using a NOx sensor cross-sensitive to NH3," *Journal of Process Control*, vol. 24, no. 2, pp. 368 – 378, 2014.

[11] A. Frobert, S. Raux, Y. Creff, and E. Jeudy, "About cross-sensitivities of NOx sensors in scr operation," in *SAE 2013 World Congress & Exhibition 2013-01-1512*. SAE International, apr 2013.

[12] D. Y. Wang, S. Yao, M. Shost, J.-H. Yoo, D. Cabush, D. Racine, R. Cloudt, and F. Willems, "Ammonia sensor for closed-loop SCR control," *SAE International Journal of Passenger Cars - Electronic and Electrical Systems 2008-01-0919*, vol. 1, pp. 323–333, apr 2008.

[13] M. Shost, J. Noetzel, M.-C. Wu, T. Sugiarto, T. Bordewyk, G. Fulks, and G. B. Fisher, "Monitoring, feedback and control of urea SCR dosing systems for NOx reduction: Utilizing an embedded model and ammonia sensing," in *SAE Technical Paper Series 2008-01-1325*. SAE International, 2008.

[14] D. Yu Wang, S. Yao, D. Cabush, and D. Racine, "Ammonia sensor for SCR NOx reduction," DELPHI, Tech. Rep., 2007.

[15] D. Blanco-Rodriguez, G. Vagnoni, and B. Holderbaum, "EU6 C-Segment Diesel vehicles, a challenging segment to meet RDE and WLTP requirements," *IFAC-PapersOnLine*, vol. 49, no. 11, pp. 649 – 656, 2016, 8th IFAC Symposium on Advances in Automotive Control AAC 2016.

[16] P. Tourlonias and G. Koltsakis, "Model-based comparative study of Euro 6 diesel aftertreatment concepts, focusing on fuel consumption," *International Journal of Engine Research*, vol. 12, no. 3, pp. 238–251, 2011.

[17] R. Cloudt, J. Saenen, E. v. d. Eijnden, and C. Rojer, "Virtual exhaust line for model-based diesel aftertreatment development," in *SAE 2010 World Congress & Exhibition 2010-01-0888*. SAE International, apr 2010.

[18] M. Devarakonda, G. Parker, J. H. Johnson, and V. Strots, "Model-based control system design in a urea-scr aftertreatment system based on nh3 sensor feedback," *International Journal of Automotive Technology*, vol. 10, no. 6, p. 653, Dec 2009.

[19] G. Cavataio, J. Girard, J. E. Patterson, C. Montreuil, Y. Cheng, and C. K. Lambert, "Laboratory testing of urea-SCR formulations to meet Tier 2 bin 5 emissions," in *SAE Technical Paper Series 2007-01-1575*. SAE International, 2007.

[20] C. Guardiola, B. Pla, J. Mora, and D. Lefebvre, "Control oriented model for diesel oxidation catalyst diagnosis," *IFAC-PapersOnLine*, vol. 48, no. 15, pp. 427 – 433, 2015.

[21] G. Hommen, F. Kupper, and X. Seykens, "Robust, model-based urea dosing control for SCR aftertreatment systems using a cross-sensitive tailpipe nox sensor," in *SAE Technical Paper Series 2017-01-0938*. SAE International, mar 2017.

[22] F. Birkhold, U. Meingast, P. Wassermann, and O. Deutschmann, "Modeling and simulation of the injection of urea-water-solution for automotive SCR DeNOx-systems," *Applied Catalysis B: Environmental*, vol. 70, no. 1, pp. 119 – 127, 2007.

[23] A. Matsumoto, K. Furui, M. Ogiso, and T. Kidokoro, "Model-based OBD logic utilizing adsorption and desorption model of NH3 in SCR catalyst," in *SAE Technical Paper 2016-01-0960*. SAE International, 04 2016.

[24] M. Colombo, I. Nova, and E. Tronconi, "Detailed kinetic modeling of the nh3-no/no2 scr reactions over a commercial cu-zeolite catalyst for diesel exhausts after treatment," *Catalysis Today*, vol. 197, no. 1, pp. 243 – 255, 2012.

[25] F. Willems and R. Cloudt, "Experimental demonstration of a new model-based scr control strategy for cleaner heavy-duty diesel engines," *IEEE Transactions on Control Systems Technology*, vol. 19, no. 5, pp. 1305–1313, 2011.

[26] D. Upadhyay and M. Van Nieuwstadt, "Modeling of urea SCR catalyst with automotive applications," 2002.

[27] I. Nova, L. Lietti, and E. Tronconi, "Transient response method applied to the kinetic analysis of the deNO x-SCR reaction," *Chemical Engineering Science*, vol. 56, no. 4, pp. 1229–1237, 2001.

[28] X. Song, J. D. Naber, and J. H. Johnson, "A study of the effects of NH3 maldistribution on a urea-selective catalytic reduction system," *International Journal of Engine Research*, vol. 16, no. 2, pp. 213–222, 2015.

[29] J. Figura, J. Pekar, P. Krejza, D. Mracek, D. von Wissel, and T. Zhang, "NO2/NOx ratio and NH3 storage estimation of automotive SCR multi-brick systems," in *SAE Technical Paper 2017-01-0972*. SAE International, 2017.

[30] T. Feng and L. Lue, "The characteristics of ammonia storage and the development of model-based control for diesel engine urea-scr system," *Journal of Industrial and Engineering Chemistry*, vol. 28, pp. 97 – 109, 2015.

[31] Q. Lin and P. Chen, "An NOx sensor-based direct algebraic approach-newton observer for urea selective catalytic reduction system state estimations," *Journal of Dynamic Systems, Measurement and Control, Transactions of the ASME*, vol. 140, no. 11, 2018.

[32] Y. Ma and J. Wang, "Observer-based estimation of aging condition for selective catalytic reduction systems in vehicle applications," *Journal of Dynamic Systems, Measurement and Control, Transactions of the ASME*, vol. 139, no. 2, 2017.

[33] M. F. Hsieh and J. Wang, "An extended kalman filter for NOx sensor ammonia cross-sensitivity elimination in selective catalytic reduction applications," in *American Control Conference (ACC), 2010*. IEEE, 2010, pp. 3033–3038.

[34] B. Jiang, Y. Hu, S. Wang, Y. Qiu, and H. Chen, "A state observer design based on EKF for diesel engine urea-SCR system," in *Proceedings of the World Congress on Intelligent Control and Automation (WCICA)*, vol. 2016-September, 2016, pp. 3324–3329.

[35] K. Jiang, H. Zhang, and J. Lin, "NH3 coverage ratio estimation of diesel-engine SCr systems by a dual time-scale extended kalman filter," *IEEE Transactions on Vehicular Technology*, vol. 67, no. 4, pp. 3625–3629, 2018.

[36] H. Zhang and J. Wang, "Adaptive sliding-mode observer design for a selective catalytic reduction system of ground-vehicle diesel engines," *IEEE/ASME Transactions on Mechatronics*, vol. 21, no. 4, pp. 2027–2038, 2016.

[37] H. Zhang, J. Wang, and Y. . Wang, "Nonlinear observer design of diesel engine selective catalytic reduction systems with nox sensor measurements," *IEEE/ASME Transactions on Mechatronics*, vol. 20, no. 4, pp. 1585–1594, 2015.

[38] H. Zhang, P. Chen, J. Wang, and Y. . Wang, "Integrated study of inland-vessel diesel engine two-cell scr systems with dynamic references," *IEEE/ASME Transactions on Mechatronics*, vol. 22, no. 3, pp. 1195–1206, 2017.

[39] H. Zhang, J. Wang, and Y. . Wang, "Sensor reduction in diesel engine two-cell selective catalytic reduction (scr) systems for automotive applications," *IEEE/ASME Transactions on Mechatronics*, vol. 20, no. 5, pp. 2222–2233, 2015.